

Detection of additional Be+sdO systems from *IUE* spectroscopy

Luqian Wang, Douglas R. Gies

*Center for High Angular Resolution Astronomy and Department of Physics and Astronomy,
Georgia State University, P. O. Box 5060, Atlanta, GA 30302-5060, USA*

lwang@chara.gsu.edu, gies@chara.gsu.edu

Geraldine J. Peters¹

*Space Sciences Center, University of Southern California, Los Angeles, CA 90089-1341,
USA*

gpeters@usc.edu

ABSTRACT

There is growing evidence that some Be stars were spun up through mass transfer in a close binary system, leaving the former mass donor star as a hot, stripped-down object. There are five known cases of Be stars with hot subdwarf (sdO) companions that were discovered through *International Ultraviolet Explorer (IUE)* spectroscopy. Here we expand the search for Be+sdO candidates using archival FUV spectra from *IUE*. We collected *IUE* spectra for 264 stars and formed cross-correlation functions (CCFs) with a model spectrum for a hot subdwarf. Twelve new candidate Be+sdO systems were found, and eight of these display radial velocity variations associated with orbital motion. The new plus known Be+sdO systems have Be stars with spectral subtypes of B0 to B3, and the lack of later-type systems is surprising given the large number of cooler B-stars in our sample. We discuss explanations for the observed number and spectral type distribution of the Be+sdO systems, and we argue that there are probably many Be systems with stripped companions that are too faint for detection through our analysis.

Subject headings: stars: emission-line, Be — stars: binaries: spectroscopic — stars: evolution — stars: subdwarfs

¹Guest Observer with the *International Ultraviolet Explorer*.

1. Introduction

Be stars are rapidly rotating B-type, non-supergiant, stars that show or have shown $H\alpha$ emission in their spectra. Their rotational velocities may reach more than 75% of the critical velocity (Slettebak 1966; Rivinius et al. 2013). Pols et al. (1991) suggested that their rapid rotation results from past mass transfer in a close binary system. The initially more massive star expands away from main-sequence stage after hydrogen core exhaustion and fills its Roche-lobe. Mass transfer from the evolved massive star to the less massive gainer star causes the latter to spin up due to conservation of angular momentum. The orbit shrinks until the two stars reach comparable masses, and then subsequent mass transfer causes the orbit to expand. This continues until the donor star loses its outer envelope and the core obtains a size smaller than the Roche-lobe. If the donor star is left with a mass above the Chandrasekhar limit, then the stars will evolve into an X-ray binary system, consisting of a Be star and a neutron star or black hole. Lower mass donor remnants become a faint, hot, subdwarf (sdO) or a white dwarf (WD).

Such sdO and WD stars are difficult to detect because they are usually lost in the glare of their massive companions and their small mass creates only a small orbital reflex motion in the Be star. The subdwarfs are hot, so it is best to search for this type of remnant in the far ultraviolet because they contribute relatively more flux there and their spectra are rich in highly ionized metallic lines. Such FUV spectroscopy investigations have led to the detection of a subdwarf companion in five systems. Thaller et al. (1995) discovered the hot subdwarf companion of ϕ Per using a Doppler tomography algorithm, which uses the radial velocities of the components to reconstruct their individual spectra. The highly ionized lines of the sdO star were clearly visible in the reconstructed secondary spectrum based on 16 Short Wavelength Prime (SWP) camera, high dispersion (H) spectra obtained with the *International Ultraviolet Explorer*. This discovery was confirmed by Gies et al. (1998) through *Hubble Space Telescope* spectroscopy, and their study suggested that the subdwarf companion has $T_{\text{eff}} = 53 \pm 3$ kK and $\log g = 4.2 \pm 0.1$. Peters et al. (2008) combined optical spectra and 96 *IUE* spectra to confirm the binarity of FY CMa, and they detected the hot companion through analysis of cross-correlation functions (CCFs) of the UV spectra with that for a hot stellar template. Their study indicated that the secondary has $T_{\text{eff}} = 45 \pm 5$ kK and $\log g = 4.3 \pm 0.6$. A similar analysis was done by Peters et al. (2013) for 59 Cyg, and they reported that the detected companion has $T_{\text{eff}} = 52.1 \pm 4.8$ kK and $\log g = 5.0 \pm 1.0$ based on a large set of 157 *IUE* spectra. Subsequently, Wang et al. (2017) analyzed 23 *IUE* spectra of 60 Cyg through CCFs with a hot stellar template, and they estimated that the hot subdwarf companion has $T_{\text{eff}} = 42 \pm 4$ kK. The fifth detection was made by Peters et al. (2016) using 88 *IUE* spectra to detect a faint signal of a hot companion in HR 2142, which indicated that the companion has $T_{\text{eff}} \geq 43 \pm 5$ kK.

The detection of the subdwarf companions of the confirmed systems benefited from the large number of observations available in the *IUE* archive in order to take advantage of the \sqrt{n} improvement in S/N by combining all the observations in the analysis. However, relatively bright subdwarf companions should be detected even in a single *IUE* observation through calculations of CCFs with a model spectrum for a hot star. The goal of this work is to detect other Be+sdO systems by searching for such relatively bright companions through analysis of individual spectra for a large sample of Be stars.

Our survey will help identify binary systems with subdwarf companions for future follow-up studies to determine the orbital and stellar parameters that are needed for critical comparisons with models for the evolution of stripped cores (Althaus et al. 2013). This survey is important for studies of massive star evolution, since a large fraction of massive stars have nearby stellar companions (Sana et al. 2012) and binary interactions play a key role in their destinies (de Mink et al. 2014). Hot evolved companions may contribute significantly to the UV flux of stellar populations (Han et al. 2010) and constitute a missing contribution to spectral synthesis models (Bruzual & Charlot 2003). Massive helium star remnants probably explode as hydrogen deficient supernovae (SN Ib and SN Ic; Eldridge et al. 2013), so a determination of their numbers and properties is closely related to the numbers and kinds of core collapse SN we observe. The rotational properties of SN progenitors dictate the spins of their neutron star and black hole remnants, and fast rotation may be responsible for the long duration γ -ray bursters that form in the core collapse of massive stars (Cantiello et al. 2007).

Here we present the results of the survey for sdO companions among rapidly rotating hot stars from an analysis of *IUE* spectra. Section 2 presents our subdwarf flux search method that is based on a cross-correlation analysis of the UV spectra with a model spectral template. We discuss the 12 new candidate Be+sdO systems in Section 3. Our final results and their consequences are summarized in Section 4.

2. Search for sdO companions

The main sample of Be stars was adopted from the list of Yudin (2001), who presented an analysis of intrinsic polarization, projected rotational velocity, and IR excess of 627 Be stars. We combed through the *IUE* archive to find these targets, and we collected 3092 SWP/H spectra of 226 stars from the archive. We further expanded the sample by adding 111 SWP/H spectra of 38 rapidly rotating, non-emission stars with projected rotational velocity $V \sin i > 300 \text{ km s}^{-1}$.

We downloaded the SWP/H spectra of these 264 stars from MAST². The spectra were reduced and rectified following the procedures reported in Wang et al. (2017), except that we left the interstellar medium lines in place. The estimated temperatures of the five known sdO companions all have $T_{\text{eff}} > 40$ kK. Thus, we adopted a synthetic spectrum with $T_{\text{eff}} = 45$ kK from the grid of Lanz & Hubeny (2003) that we used earlier (Wang et al. 2017), and we cross-correlated it with all the observed spectra. We excluded the beginning and ending regions and very broad or blended line regions (including the Si III λ 1300 complex, Si IV λ 1394, 1403, Si II λ 1527, 1533, and C IV λ 1550) that were replaced by a linear interpolation across the adjacent continuum to avoid introduction of broad features into the CCFs.

We began our search for hot companions by forming the ratio of the CCF maximum height (peak signal S) within a velocity range of ± 200 km s⁻¹ (larger than the typical span of Doppler shift of the known binaries) to the standard deviation of the CCF in higher velocity portions (background noise N), and we then calculated the average peak-to-background ratio (S/N) from the individual ratios for all the available spectra for each star. The average S/N ratios of the known Be+sdO systems (ϕ Per, FY CMa, 59 Cyg, and 60 Cyg) all have S/N > 3.0. Thus, we set this CCF peak-to-background ratio as the lower limit to select candidate sdO binaries. Null detections of companion stars with CCF S/N ratios below the selection criterion are listed in Table 1. If the stars in Table 1 host hot companions, then their sdO components must be too faint to detect in individual *IUE* spectra. Table 1 includes HR 2142 (=HD 41335), which only displays the weak signal of the companion in a subset of spectra (Peters et al. 2016). On the other hand, a strong signal appeared and met the selection criterion for 66 stars, forming a preliminary list of potential binary systems with relatively bright subdwarf companions. We collected the spectral classifications and projected rotational velocities of these targets from the literature. The HD number, star name, HIP number, spectral classification, projected rotational velocity, number of SWP/H spectra available in the *IUE* archive, average CCF S/N ratio, and references for the spectral types and $V \sin i$ are tabulated in Table 2.

We adopted detection criteria for Be+sdO binaries that are based upon the characteristics of the five known systems. The best known system (and the one with the highest CCF S/N ratio in our sample) is ϕ Per (HD 10516), and we show in Figure 1, top left panel, two CCFs for ϕ Per at different orbital velocity extrema. The CCF peaks are narrow (indicative of a small projected rotational velocity) and show large velocity excursions due to the large semi-amplitude associated with the low mass sdO star (Gies et al. 1998). All five known Be+sdO binaries share these properties, so we adopted two detection criteria based upon

²<https://archive.stsci.edu/iue/>

them.

The first criterion is that any CCF signal from the sdO component must be narrow with a half width at half maximum (HWHM) much smaller than the projected rotational broadening $V \sin i$ associated with the primary Be star target. Most Be stars are rapid rotators with large $V \sin i$, so their associated CCFs are very broad (see the case of γ Cas = HD 5394 in the lower left panel of Fig. 1), although a few pole-on Be stars do show smaller projected rotational broadening (see the CCFs of HD 120991 in the lower, right panel of Fig. 1). Note that this assumption biases the results against detection of rapidly rotating sdO components, but we doubt such exist in general because their progenitors probably became synchronous rotators in long period orbits during the earlier mass transfer phase. Note that the CCF signal from correlation with the Be star spectral features will become larger for hotter Be stars, so that the CCF will be more dominated by the Be star signal in earlier-type targets. We show, for example, the cases of CCFs for a hot (HD 155806) and a mid-temperature (HD 174237) emission-line star in the middle left and right panels, respectively, of Figure 1. The sensitivity of the CCFs to the temperature of the Be star means that it will become progressively more difficult to distinguish the signal from a sdO component from that of the Be star at high temperature, so our methods may be biased against detection of sdO companions among the hotter Be stars. Nevertheless, it is possible to discern the narrow sdO component against broader Be component in some cases of hotter Be stars (see the case of FY CMa = HD 53978 in the upper right panel of Fig. 1, which shows the narrow peak of the sdO star atop the broader signal from the Be star).

The second criterion is based upon the expected orbital motion of the sdO component. Post-mass transfer binaries are expected to have extreme mass ratios, so that the orbital semiamplitudes of the sdO components will be large ($\approx 50 - 100 \text{ km s}^{-1}$) compared to those of the Be stars ($< 10 \text{ km s}^{-1}$) for binaries with periods of a few months or less. Thus, our second criterion for sdO candidates is that their CCF signals should show a velocity range greater than 1/2 of the HWHM of the CCF peak. This criterion tacitly assumes that enough spectra exist to sample the full range of orbital motion, but this cannot be fulfilled in cases where only a few spectra are available. Note that application of this criterion will impose a bias against detection of binaries in low inclination and long period orbits (with small orbital semiamplitude).

The results of applying these two detection criteria are summarized in a code in the last column of Table 2. We find that 50 of the 66 targets in the list of large S/N cases are best explained as the result of correlation with the Be star spectrum itself (indicated by a “P” for primary in Table 2). These are generally hotter Be stars in which the CCF signal has a half-width comparable to the published $V \sin i$, and their CCF peaks show little evidence

of significant orbital Doppler shifts. Some of these cases are discussed in the Appendix. Next, the application of the two criteria led to the successful re-identification of four known Be+sdO binaries (ϕ Per, FY CMa, 59 Cyg, and 60 Cyg), and these are indicated by an “S” (for subdwarf) in Table 2. The criteria also led to the detection of eight additional candidate Be+sdO binaries that are labeled with a “C” in Table 2. Finally, we list four systems in which a strong and narrow CCF peak was found, but only one or two spectra are available in the *IUE* archive so that we could not apply the second criterion of velocity variability. These four potential candidates are indicated by a “C?” code in Table 2. Radial velocities from Gaussian fits of the upper 80% of the CCF peaks are listed in Table 3 for these eight candidate and four potential candidate systems, but measurements from noisy spectra with weak CCF signals were omitted. The number and time distribution of these measurements are insufficient to find orbital periods and other elements, but they are included here for future use once orbits are determined (perhaps by ground-based spectroscopy of the Be components). All these new detections are discussed further in the next section.

3. Candidate Be+sdO systems

We identified twelve subdwarf candidates from the CCF analysis that display a narrow peak as expected from correlation with the hot subdwarf spectrum template. We observe significant Doppler shift variations in the CCF signals of eight systems due to the orbital motion of the subdwarf companion. Figure 2 shows the apparent CCFs of the eight candidate systems for spectra observed near the velocity extrema (see Table 3). The remaining four potential subdwarf candidates in the sample display a narrow peak, but little or no information about their Doppler shifts is available due to the limited number of spectra available. The CCFs for these four cases are shown in Figure 3. The peak height of the CCF scales approximately with the subdwarf flux contribution if the model template is a reasonable match (Wang et al. 2017), so the new candidates contribute about 2 – 5% of the FUV monochromatic flux (and probably less at optical wavelengths).

None of the candidates are known close binaries, but all are worthy of follow-up investigation. We summarize a brief literature review for each candidate below. Many of the candidate Be+sdO systems have additional companions detected through speckle interferometry or optical imaging, but their orbital periods must be decades or longer. Consequently these visually resolved companions are unrelated to the subdwarf companions that are the remnants of interactions in close binaries. The speckle interferometry observations reveal companions in the angular separation range of $0.035 < \rho < 1''.5$ and brighter than $\Delta m < 3.0$ mag (Mason et al. 1997).

HD 29441 (V1150 Tau; B2.5 Vne; S/N = 3.77). Based on measurements of six optical spectra, Chini et al. (2012) found that the star is radial velocity constant, perhaps indicating that the sdO is a low mass object or that the orbit is very long.

HD 43544 (B3 V; S/N = 5.51). Huang et al. (2010) argued that the star had a significant radial velocity shift between measurements of two optical spectra, indicative of the orbital motion of the Be star. No other companions have been detected through speckle interferometry from Mason et al. (1997).

HD 51354 (QY Gem; B3 Ve; S/N = 5.39). Chojnowski et al. (2017) observed only a small scatter of 3.0 km s^{-1} in six radial velocity measurements from the APOGEE survey.

HD 60855 (V378 Pup; B3 IV; S/N = 4.98). The CCFs of the star display a narrow central peak that sits atop a broader signal from the Be star. The measured velocities from the CCFs of the six available spectra did not display large velocity shifts, perhaps indicating that the sdO is in a long period, slow moving orbit. However, Huang & Gies (2006) found a significant velocity shift between their two spectra indicative of possible orbital motion of the Be star. Mason et al. (1997) found no evidence from speckle interferometry for another companion in the separation range of 0.04 to 1 arcsec. Mason et al. (2001) note that this star is a member of the NGC 2422 cluster, and the nearest companion has separation of 5.3 arcsec from the star.

HD 113120 (LS Mus; B2 IVne; S/N = 4.35). Based on spectroscopic measurements from five optical spectra, Chini et al. (2012) found that the star is radial velocity constant, which suggests a small orbital semi-amplitude for the Be star. Nevertheless, we observe relatively large Doppler shifts for the sdO component. Hartkopf et al. (1996) detected a companion with angular separation of 0.557 arcsec from the star through speckle interferometry.

HD 137387 (κ^1 Aps; B2 Vnpe; S/N = 5.21). Lindroos (1985) reported that the star belongs to a visual binary system with a companion of estimated spectral type of K7 IV and a projected separation of 1470 AU from the star.

HD 152478 (V846 Ara; B3 Vnpe; S/N = 3.69). Hoogerwerf et al. (2001) mention this object as a possible runaway star. de Bruijne & Eilers (2012) list a radial velocity of 19 km s^{-1} .

HD 157042 (ι Ara; B2.5 IVe; S/N = 4.09). Based on optical studies, Lindroos (1985) reported that the star has a companion with estimated spectral type of G5 III-IV and a separation of 42.8 arcsec from the primary component.

HD 157832 (V750 Ara; B1.5 Ve; S/N = 4.21). Based on observations from XMM-Newton and optical spectroscopy, Lopes de Oliveira & Motch (2011) classified the star as the coolest γ Cas analogue. Based on the presence of Fe XXI and Fe XXII recombination lines and fluorescence features, Giménez-García et al. (2015) confirmed the X-ray properties of the star and classified it as a component of high-mass X-ray binary.

HD 191610 (28 Cyg; B3 IVe; S/N = 3.02). Abt & Levy (1978) reported that the star is radial velocity constant from spectroscopic studies based on 25 optical spectra. Based on an analysis of space photometry and H α line profiles, Baade et al. (2017) concluded that the large-amplitude frequencies due to multiple non-radial pulsation modes are responsible for the observed short- and medium-term variability, and these pulsation modes are also related to the modulation of mass transfer events from the star to the disk of 28 Cyg. No other companions have been found by Mason et al. (1997) through speckle interferometry.

HD 194335 (V2119 Cyg; B2 IIIe; S/N = 4.54). The star is listed as a shell star by Hoffleit & Jaschek (1991). Plaskett et al. (1920) suggested that the object is a possible spectroscopic binary.

HD 214168 (8 Lac B; B1 IVe; S/N = 3.03). Hoffleit & Jaschek (1991) also identified this star as a shell star. It is a member of the Lac OB1 association. Mason et al. (1997) identified a companion with an angular separation of 0.042 arcsec using speckle interferometry. Shatskii (1998) and Mason et al. (2007) confirmed that the star forms a double system with HD 214167 (B1.5 Vs) with an angular separation of 22.24 arcsec.

4. Conclusions

We identified eight subdwarf candidates and four potential candidates, and by including the five Be+sdO systems known from previous studies, this leads to a total of 17 detections in the sample of 264 stars, for a detection rate of 6%. The CCF S/N ratios have a range between 3.0 and 5.5 with a mean of 4.3, and these ratios are generally less than or comparable to those of the known systems. The distributions with spectral type of the known plus candidate targets and of the full sample are shown in Figure 4. Most of the new candidates have spectral types of B2-B3, which are relatively cooler compared to the primaries of the known Be+sdO systems with spectral types of B0.5-B1.5. However, we found no companions among the cooler, later-type B-stars, despite the fact that such hot companions should be more readily detected as they dominate more of the FUV flux distribution relative to cooler, main sequence companions. There are 109 targets with spectral types B4 and later in our sample (41%). If the Be+sdO systems had the same spectral type distribution as the whole sample, then we would expect to have found 7 of 17 systems among the B4-A0 group, yet none were detected.

Binary star population models make different predictions about the numbers of expected Be+He star systems (which we may compare to the observed Be+sdO systems) as a function of Be star mass or spectral type. High mass He star remnants have relatively shorter lives, so the numbers of such systems are predicted to decline with higher Be star mass. On the

other hand, lower mass remnants above the He-burning limit ($\approx 0.3M_{\odot}$) will have He-burning lifetimes longer than those of the rejuvenated gainer stars, so many lower mass Be stars could have He star companions. However, the expected numbers depend critically on assumptions about the initial mass ratio distribution of the binaries and which systems merge during interaction. Pols et al. (1991) show in their Figure 10(b) the numbers of Be+He systems expected for a magnitude limited sample like the Bright Star Catalogue (Hoffleit & Jaschek 1991). If the initial mass ratio distribution is flat, then the numbers of Be+He systems peak in the B0-B5 range, because there are relatively fewer low mass systems. However, for initial mass ratio distributions that favor lower mass companions, the relative numbers of low mass Be+He systems increase. This is also seen in the simulations by Shao & Li (2014) who find the largest numbers of Be+He systems (in a volume limited sample) among the latest B-types when the assumed initial mass ratio distribution is highly skewed to low mass companions (numbers proportional to $(M_2/M_1)^{-1}$; see their Fig. 7). The observed lack of Be+sdO companions among the late-type B-stars in our sample would appear to favor progenitor systems with a flat initial mass ratio distribution.

The low-mass, rapid rotators that comprise the late-type Be stars may be the result of mergers that occur more frequently among lower mass systems (Shao & Li 2014) or they may result from extreme mass transfer that creates low mass cores that quickly cool to become helium white dwarfs (Chen et al. 2017). Such low mass white dwarfs are now known to orbit some late B-type, rapid rotators including Regulus ($0.3M_{\odot}$; Gies et al. 2008), KOI-81 ($0.2M_{\odot}$; Matson et al. 2015), and possibly β CMi ($0.4M_{\odot}$; Dulaney et al. 2017).

If binary mass transfer is a significant mechanism in the production of Be stars, then we need to consider why hot companions are not found for all the B0-B3 stars in our sample. We suspect that many such companions spend much of their lives with a luminosity that is too low for detection by our methods. For example, Schootemeijer et al. (2017) present a path in the H-R diagram for the stripped remnant of HD 10516 (ϕ Per) based on He star evolutionary models. They argue that the subdwarf companions in ϕ Per, FY CMa, and 59 Cyg are most likely experiencing a helium shell burning stage, in which the core has finished helium burning and the star swells to increased luminosity. This phase lasts about 10% of the total post-mass transfer lifetime. Thus, we expect that those stars that are bright enough to detect in our survey are representative of this advanced He-shell burning stage. The fraction of detected companions in B0-B3 range ($17/140 = 12\%$) is close to the typical fraction of time spent in He-shell burning phase. On the other hand, 90% of the post-mass transfer lifetime is spent in the prior He-core burning stage, during which the subdwarfs have lower luminosity. These faint sdO companions are very difficult to detect unless a large set of spectra is available to reveal the orbital motion (for example, the case of HR 2142; Peters et al. 2016). Consequently, it is possible that many or most of the B0-B3

stars in our sample do have sdO companions that are undetected because they are faint, He-core burning objects. Long term radial velocity and orbital-phase related emission line monitoring (Koubský et al. 2012) may prove to be effective ways to discover their binary properties.

We thank Dr. Michael Crenshaw for helping us interpret the radial velocity shifts apparent in some of the *IUE* spectra, and we thank an anonymous referee for their insight about the spectral subtype distribution of the sample. The data presented in this paper were obtained from the Mikulski Archive for Space Telescopes (MAST). STScI is operated by the Association of Universities for Research in Astronomy, Inc., under NASA contract NAS5-26555. Support for MAST for non-HST data is provided by the NASA Office of Space Science via grant NNX09AF08G and by other grants and contracts. Our work was supported in part by NASA grant NNX10AD60G (GJP) and by the National Science Foundation under grant AST-1411654 (DRG). Institutional support has been provided from the GSU College of Arts and Sciences, the Research Program Enhancement fund of the Board of Regents of the University System of Georgia (administered through the GSU Office of the Vice President for Research and Economic Development), and by the USC Women in Science and Engineering (WiSE) program (GJP).

Facilities: IUE

A. Notes on individual stars

HD 35411 (η Ori; B1 IV). Zizka & Beardsley (1981) measured the spectroscopic radial velocities of the inner binary system and concluded that the Aa1, Aa2 pair has an orbital period of 7.989 d. The first speckle measurements done by McAlister (1976) showed that there is a third star (B3 IV) that orbits around the inner eclipsing and spectroscopic binary system Aa1, Aa2 (B1 IV and B3 IV, respectively) in an orbit with an angular semimajor axis of 44 mas and a period of 9.2 yr. The *IUE* spectra recorded the flux of all three components. The cross-correlation functions of the spectra show a sharp peak, and the peak half-width is comparable to the projected rotational velocity of Aa1. Furthermore, the measured CCF peak velocities appear to match the Aa1 radial velocity curve from De Mey et al. (1996) in their Figure 3. Thus, we conclude that the CCF peaks result from correlation with the spectral features of the primary Aa1 component of the inner binary system.

HD 53367 (V750 Mon; B0 IVe). Based on spectroscopic studies of the optical lines, Pogodin et al. (2006) proposed that the system consists of a primary main-sequence star ($\sim 20M_{\odot}$) and a pre-main sequence secondary ($\sim 5M_{\odot}$). We compared the measured peak velocities with the primary radial velocity curve in Figure 6 of Pogodin et al. (2006), and the similarity of the velocities suggests that the CCF peak is mostly due to correlation with the spectral features of the primary component. However, we noticed that two spectra (SWP38685 and SWP38686) yielded a peak velocity variation of $\sim 50 \text{ km s}^{-1}$ in less than 3 hours. We examined the spectra and found that the star drifted in position across the dispersion in the large aperture of the camera between exposures. Thus, this rapid velocity variation is instrumental in origin.

HD 135160 (B0 IV). The CCFs show both a sharp peak and an extended wing feature that varies in velocity. Chini et al. (2012) detected spectral lines of both components of this suspected spectroscopic binary. The Doppler shifts apparent in the CCFs tend to confirm the spectroscopic binary nature of the system.

HD 166596 (V692 CrA; B2.5 IIIp). *IUE* recorded two spectra of this star within ~ 1 hour. The peak velocities of the CCFs indicate a significant shift of $\sim 37 \text{ km s}^{-1}$ between the observations. Renson & Manfroid (2009) report that the target is a silicon star with a rotational period of ~ 1.7 d. We suggest that the rapid velocity variation is probably related to rotational Doppler shifts of regions with chemical peculiarities.

HD 178175 (V4024 Sgr; B2 IV(e)). The CCFs show a sharp peak. Based on spectroscopic studies, Bragança et al. (2012) reported that the star has $V \sin i = 86 \text{ km s}^{-1}$, similar to the half-width of the CCF peak. However, Bragança et al. (2012) estimate that the star’s temperature is $T_{\text{eff}} = 19.6 \text{ kK}$, and we would usually expect little correlation with the features of such a relatively cooler object. However, the CCFs show no significant peak velocity variations. Thus, we conclude that the CCFs are most likely due to correlation with

the features of the Be star that are narrow enough in this case to produce a detectable CCF peak.

REFERENCES

- Abt, H. A., Levato, H., & Grosso, M. 2002, *ApJ*, 573, 359
- Abt, H. A., & Levy, S. G. 1978, *ApJS*, 36, 241
- Althaus, L. G., Miller Bertolami, M. M., & Córscico, A. H. 2013, *A&A*, 557, A19
- Baade, D., Pigulski, A., Rivinius, T., et al. 2017, *A&A*, submitted (arXiv 1708.07360)
- Bragança, G. A., Daflon, S., Cunha, K., et al. 2012, *AJ*, 144, 130
- Bruzual, G., & Charlot, S. 2003, *MNRAS*, 344, 1000
- Cantiello, M., Yoon, S.-C., Langer, N., & Livio, M. 2007, *A&A*, 465, L29
- Chen, X., Maxted, P. F. L., Li, J., & Han, Z. 2017, *MNRAS*, 467, 1874
- Chini, R., Hoffmeister, V. H., Nasserri, A., Stahl, O., & Zinnecker, H. 2012, *MNRAS*, 424, 1925
- Chojnowski, S. D., Wisniewski, J. P., Whelan, D. G., et al. 2017, *AJ*, 153, 174
- de Bruijne, J. H. J., & Eilers, A.-C. 2012, *A&A*, 546, A61
- De Mey, K., Aerts, C., Waelkens, C., & Van Winckel, H. 1996, *A&A*, 310, 164
- de Mink, S. E., Sana, H., Langer, N., Izzard, R. G., & Schneider, F. R. N. 2014, *ApJ*, 782, 7
- Dulaney, N. A., Richardson, N. D., Gerhartz, C. J., et al. 2017, *ApJ*, 836, 112
- Eldridge, J. J., Fraser, M., Smartt, S. J., Maund, J. R., & Crockett, R. M. 2013, *MNRAS*, 436, 774
- Frémat, Y., Zorec, J., Hubert, A.-M., & Floquet, M. 2005, *A&A*, 440, 305
- Gies, D. R., Bagnuolo, Jr., W. G., Ferrara, E. C., et al. 1998, *ApJ*, 493, 440
- Gies, D. R., Dieterich, S., Richardson, N. D., et al. 2008, *ApJ*, 682, L117
- Giménez-García, A., Torrejón, J. M., Eikmann, W., et al. 2015, *A&A*, 576, A108
- Han, Z., Podsiadlowski, P., & Lynas-Gray, A. 2010, *Ap&SS*, 329, 41
- Hartkopf, W. I., Mason, B. D., McAlister, H. A., et al. 1996, *AJ*, 111, 936

- Hoffleit, D., & Jaschek, C. 1991, *The Bright Star Catalogue* (5th ed.; New Haven, CT: Yale University Observatory)
- Hoogerwerf, R., de Bruijne, J. H. J., & de Zeeuw, P. T. 2001, *A&A*, 365, 49
- Houk, N. 1978, *Michigan Catalogue of Two-dimensional Spectral Types for the HD stars. Declinations -52 to -41 , Vol. 2* (Ann Arbor, MI: University of Michigan)
- . 1982, *Michigan Catalogue of Two-dimensional Spectral Types for the HD stars. Declinations -40 to -26 , Vol. 3* (Ann Arbor, MI: University of Michigan)
- Houk, N., & Cowley, A. P. 1975, *Michigan Catalogue of Two-dimensional Spectral Types for the HD stars. Declinations -90 to -53 , Vol. 1* (Ann Arbor, MI: University of Michigan)
- Houk, N., & Swift, C. 1999, *Michigan Catalogue of Two-dimensional Spectral Types for the HD stars. Declinations -12 to 5 , Vol. 5* (Ann Arbor, MI: University of Michigan)
- Huang, W., & Gies, D. R. 2006, *ApJ*, 648, 580
- Huang, W., Gies, D. R., & McSwain, M. V. 2010, *ApJ*, 722, 605
- Koubský, P., Kotková, L., Votruba, V., Šlechta, M., & Dvořáková, Š. 2012, *A&A*, 545, A121
- Koubský, P., Harmanec, P., Hubert, A. M., et al. 2000, *A&A*, 356, 913
- Lanz, T., & Hubeny, I. 2003, *ApJS*, 146, 417
- Lesh, J. R. 1968, *ApJS*, 17, 371
- Levenhagen, R. S., & Leister, N. V. 2006, *MNRAS*, 371, 252
- Lindroos, K. P. 1985, *A&AS*, 60, 183
- Lopes de Oliveira, R., & Motch, C. 2011, *ApJ*, 731, L6
- Mason, B. D., Hartkopf, W. I., Wycoff, G. L., & Wieder, G. 2007, *AJ*, 134, 1671
- Mason, B. D., ten Brummelaar, T., Gies, D. R., Hartkopf, W. I., & Thaller, M. L. 1997, *AJ*, 114, 2112
- Mason, B. D., Wycoff, G. L., Hartkopf, W. I., Douglass, G. G., & Worley, C. E. 2001, *AJ*, 122, 3466
- Matson, R. A., Gies, D. R., Guo, Z., et al. 2015, *ApJ*, 806, 155

- Mayer, A., Deschamps, R., & Jorissen, A. 2016, *A&A*, 587, A30
- McAlister, H. A. 1976, *PASP*, 88, 957
- Peters, G. J., Gies, D. R., Grundstrom, E. D., & McSwain, M. V. 2008, *ApJ*, 686, 1280
- Peters, G. J., Pewett, T. D., Gies, D. R., Touhami, Y. N., & Grundstrom, E. D. 2013, *ApJ*, 765, 2
- Peters, G. J., Wang, L., Gies, D. R., & Grundstrom, E. D. 2016, *ApJ*, 828, 47
- Plaskett, J. S., Harper, W. E., Young, R. K., & Plaskett, H. H. 1920, *Publications of the Dominion Astrophysical Observatory Victoria*, 1, 163
- Pogodin, M. A., Drake, N. A., Jilinski, E. G., et al. 2012, in *Circumstellar Dynamics at High Resolution*, ASP Conf. Vol. 464, ed. A. C. Carciofi & T. Rivinius (San Francisco, CA: ASP), 227
- Pogodin, M. A., Malanushenko, V. P., Kozlova, O. V., Tarasova, T. N., & Franco, G. A. P. 2006, *A&A*, 452, 551
- Pols, O. R., Cote, J., Waters, L. B. F. M., & Heise, J. 1991, *A&A*, 241, 419
- Renson, P., & Manfroid, J. 2009, *A&A*, 498, 961
- Rivinius, T., Carciofi, A. C., & Martayan, C. 2013, *A&A Rev.*, 21, 69
- Sana, H., de Mink, S. E., de Koter, A., et al. 2012, *Science*, 337, 444
- Schootemeijer, A., Götberg, Y., de Mink, S. E., Gies, D., & Zapartas, E. 2017, *A&A*, submitted
- Shao, Y., & Li, X.-D. 2014, *ApJ*, 796, 37
- Shatskii, N. I. 1998, *Astronomy Letters*, 24, 257
- Simón-Díaz, S., & Herrero, A. 2014a, *A&A*, 562, A135
- . 2014b, *A&A*, 562, A135
- Slettebak, A. 1966, *ApJ*, 145, 126
- . 1982, *ApJS*, 50, 55
- Thaller, M. L., Bagnuolo, Jr., W. G., Gies, D. R., & Penny, L. R. 1995, *ApJ*, 448, 878

Uesugi, A., & Fukuda, I. 1970, Catalogue of rotational velocities of the stars (Kyoto: University of Kyoto)

Wang, L., Gies, D. R., & Peters, G. J. 2017, *ApJ*, 843, 60

Yudin, R. V. 2001, *A&A*, 368, 912

Zizka, E. R., & Beardsley, W. R. 1981, *AJ*, 86, 1944

Table 1. Stars with CCF S/N < 3

Name	Name	Name	Name	Name
144	4180	6811	10144	11415
11946	13268	14434	15642	18552
20340	21362	21551	22192	22780
23016	23302	23383	23478	23480
23552	23630	23862	24479	25940
26356	26670	26793	28459	28867
29866	32343	32990	32991	33599
34863	34959	35407	35439	36012
36408	36665	36939	37115	37202
37397	37795	37967	38087	38831
41335*	42054	42545	44458	44506
45314	45542	45725	45910	45995
46056	46485	47054	47359	50123
50820	51480	52356	52721	56139
57150	58343	58715	60606	61355
63462	65875	69106	69404	70084
71216	72014	72067	75311	75416
76534	77366	79351	83953	86612
87543	87901	89080	89884	89890
91120	91465	92938	93563	100673
100889	102776	105382	107348	109387
109857	110335	110432	110863	112078
112091	118246	119921	121847	124367
127973	130109	134481	135734	137432
138749	138769	139431	141637	142184
142926	142983	149485	149671	149757
155896	156468	158427	158643	160202
162732	164284	164906	165063	166014
167128	168957	169033	171406	174639
175869	177724	178475	179343	181615
182180	183133	183362	183656	183914
185037	187235	187811	189687	191423
192044	192685	192954	193182	193911
195325	198183	198625	199218	202904
203064	203467	203699	204860	205637
206773	208057	208392	208682	208886
209014	209409	209522	210129	214748
216200	217050	217086	217543	217676
217891	218393	218674	219688	224686
BD+41 3731	BD+60 594	BD+34 1058		

*HR 2142 has a faint sdO companion (Peters et al. 2016).

Note. — Stars are listed by HD number, except for the last three.

Table 2. *IUE* Observations of sample stars

HD Number	Star Name	HIP Number	Spectral Classification	$V \sin i$ (km s ⁻¹)	Number of Observations	S/N Ratio	Spectral classification Reference	$V \sin i$ Reference	CCF Code ^a
Candidate and Known Be+sdO Systems									
10516	ϕ Per	8068	B1.5 V:e-shell	440	16	6.78	Slettebak (1982)	Frémat et al. (2005)	S
29441	V1150 Tau	21626	B2.5 Vne	311	1	3.77	Yudin (2001)	Yudin (2001)	C?
43544	...	29771	B3 V	256	1	5.51	Slettebak (1982)	Bragança et al. (2012)	C?
51354	QY Gem	33493	B3 Ve	306	2	5.39	Slettebak (1982)	Yudin (2001)	C?
58978	FY CMa	36168	B0.5 IVe	340	96	3.10	Slettebak (1982)	Peters et al. (2008)	S
60855	V378 Pup	36981	B3 IV	239	6	4.98	Slettebak (1982)	Frémat et al. (2005)	C
113120	LS Mus	63688	B2 IVne	307	3	4.35	Levenhagen & Leister (2006)	Yudin (2001)	C
137387	κ^1 Aps	76013	B2 Vnpe	250	4	5.21	Levenhagen & Leister (2006)	Frémat et al. (2005)	C
152478	V846 Ara	82868	B3 Vnpe	340	2	3.69	Levenhagen & Leister (2006)	Pogodin et al. (2012)	C
157042	ι Ara	85079	B2.5 IVe	340	4	4.09	Slettebak (1982)	Frémat et al. (2005)	C
157832	V750 Ara	85467	B1.5 Ve	266	2	4.21	Lopes de Oliveira & Motch (2011)	Lopes de Oliveira & Motch (2011)	C?
191610	28 Cyg	99303	B3 IVe	300	46	3.02	Slettebak (1982)	Frémat et al. (2005)	C
194335	V2119 Cyg	100574	B2 IIIe	360	4	4.54	Slettebak (1982)	Frémat et al. (2005)	C
200120	59 Cyg	103632	B1 Ve	379	193	3.34	Slettebak (1982)	Frémat et al. (2005)	S
200310	60 Cyg	103732	B1 Ve	320	23	4.69	Koubský et al. (2000)	Koubský et al. (2000)	S
214168	8 Lac B	111544	B1 IVe	300	20	3.03	Slettebak (1982)	Frémat et al. (2005)	C
Other Stars									
5394	γ Cas	4427	B0.5 IVe	432	227	3.81	Slettebak (1982)	Frémat et al. (2005)	P
20336	BK Cam	15520	B2 (IV:)e	328	2	3.31	Slettebak (1982)	Frémat et al. (2005)	P
24534	X Per	18350	O9.5 III	293	43	3.75	Slettebak (1982)	Frémat et al. (2005)	P
28497	DU Eri	20922	B1 Ve	300	28	3.01	Slettebak (1982)	Frémat et al. (2005)	P
30076	DX Eri	22024	B2 Ve	168	24	3.30	Slettebak (1982)	Huang et al. (2010)	P
33328	λ Eri	23972	B2 III(e)p	318	146	3.35	Slettebak (1982)	Frémat et al. (2005)	P
35411	η Ori	25281	B1 V	20	19	10.28	Slettebak (1982)	De Mey et al. (1996)	P
36576	V960 Tau	26064	B1.5 IVe	265	11	3.14	Slettebak (1982)	Frémat et al. (2005)	P
37490	ω Ori	26594	B3 Ve	171	190	3.43	Levenhagen & Leister (2006)	Yudin (2001)	P
37674	...	26683	B5 V(n)	...	1	3.34	Houk & Swift (1999)	...	P
48917	FT CMa	32292	B2 V	205	5	3.48	Houk (1982)	Frémat et al. (2005)	P
50013	κ CMa	32759	B2 IVe	243	3	4.55	Slettebak (1982)	Frémat et al. (2005)	P
50083	V742 Mon	32947	B2 Ve	170	2	3.90	Yudin (2001)	Frémat et al. (2005)	P
52918	19 Mon	33971	B2 Vn(e)	265	15	3.10	Houk & Swift (1999)	Huang et al. (2010)	P
53367	V750 Mon	34116	B0 IVe	86	4	11.05	Pogodin et al. (2006)	Yudin (2001)	P
54309	FV CMa	34360	B2 IVe	195	2	3.63	Slettebak (1982)	Frémat et al. (2005)	P

Table 2—Continued

HD Number	Star Name	HIP Number	Spectral Classification	$V \sin i$ (km s ⁻¹)	Number of Observations	S/N Ratio	Spectral classification Reference	$V \sin i$ Reference	CCF Code ^a
56014	EW CMa	34981	B3 III(e)p-shell	280	12	3.45	Slettebak (1982)	Frémat et al. (2005)	P
58050	OT Gem	35933	B2 Ve	130	4	3.65	Yudin (2001)	Frémat et al. (2005)	P
60848	BN Gem	37074	O8 Vpe	247	13	4.05	Yudin (2001)	Frémat et al. (2005)	P
66194	V374 Car	38994	B2.5 IVe	224	2	3.27	Slettebak (1982)	Yudin (2001)	P
67536	V375 Car	39530	B2 Vn	292	22	3.28	Houk & Cowley (1975)	Uesugi & Fukuda (1970)	P
68980	MX Pup	40274	B1.5 IVe	145	3	4.91	Slettebak (1982)	Frémat et al. (2005)	P
74455	HX Vel	42712	B2/3 IV/V	285	7	4.56	Houk (1978)	Uesugi & Fukuda (1970)	P
74753	D Vel	42834	B1/2 II/III(n)	288	1	3.47	Houk (1978)	Uesugi & Fukuda (1970)	P
78764	E Car	44626	B2 IVe	127	3	5.42	Slettebak (1982)	Yudin (2001)	P
88661	QY Car	49934	B2 IVe	237	14	3.71	Slettebak (1982)	Frémat et al. (2005)	P
93030	θ Car	52419	B0 Vp	145	33	8.68	Yudin (2001)	Yudin (2001)	P
96864	B1.5 IVnep	...	1	4.16	Yudin (2001)	...	P
105435	δ Cen	59196	B2 IVe	260	19	3.35	Slettebak (1982)	Frémat et al. (2005)	P
116781	V967 Cen	65637	B0 IIIne	...	1	7.55	Yudin (2001)	...	P
120324	μ Cen	67472	B2 Vnpe	159	36	4.62	Levenhagen & Leister (2006)	Frémat et al. (2005)	P
120991	V767 Cen	67861	B2 IIIep	70	5	6.09	Slettebak (1982)	Frémat et al. (2005)	P
135160	...	74750	B0 V	155	3	7.00	Slettebak (1982)	Yudin (2001)	P
148184	χ Oph	80569	B1.5 Ve	144	10	4.87	Slettebak (1982)	Frémat et al. (2005)	P
153261	V828 Ara	83323	B2 IVe	184	1	3.92	Yudin (2001)	Yudin (2001)	P
155806	V1075 Sco	84401	O7.5 IIIe	116	6	9.96	Slettebak (1982)	Yudin (2001)	P
166596	V692 CrA	89290	B2.5 IIIp	207	2	3.20	Yudin (2001)	Frémat et al. (2005)	P
170235	V4031 Sgr	90610	B1 Vnne	163	2	4.39	Levenhagen & Leister (2006)	Yudin (2001)	P
173219	V447 Sct	91946	B0 Iae	...	3	4.15	Houk & Swift (1999)	...	P
173948	λ Pav	92609	B2 Ve	140	5	5.09	Levenhagen & Leister (2006)	Frémat et al. (2005)	P
174237	CX Dra	92133	B4 IV(e)	163	64	3.16	Slettebak (1982)	Frémat et al. (2005)	P
178175	V4024 Sgr	93996	B2 V(e)	86	6	5.51	Slettebak (1982)	Bragança et al. (2012)	P
184279	V1294 Aql	96196	B0 V	212	11	3.39	Levenhagen & Leister (2006)	Yudin (2001)	P
184915	κ Aql	96483	B0.5 III	284	4	3.38	Slettebak (1982)	Simón-Díaz & Herrero (2014a)	P
187567	V1339 Aql	97607	B2.5 IVe	140	3	3.26	Yudin (2001)	Abt et al. (2002)	P
188439	V819 Cyg	97845	B0.5 III(n)	299	1	3.75	Lesh (1968)	Simón-Díaz & Herrero (2014b)	P
203374	...	105250	B0 IVpe	342	1	3.76	Yudin (2001)	Frémat et al. (2005)	P
212044	V357 Lac	110287	B0 Ve	162	1	4.33	Yudin (2001)	Yudin (2001)	P
212076	31 Peg	110386	B1.5 Ve	98	6	3.95	Slettebak (1982)	Frémat et al. (2005)	P
212571	π Aqr	110672	B1 Ve	230	21	3.18	Mayer et al. (2016)	Frémat et al. (2005)	P

^aS = known Be+sdO binary; C = candidate binary; C? = potential candidate binary; P = CCF signal from primary star.

Table 3. Radial Velocity Measurements of Candidate sdO Components

HD Number	Date (HJD-2400000)	SWP Number	V_{peak} (km s^{-1})	σ (km s^{-1})
29441	49651.9145	52665	-60.7	2.5
43544	45698.7251	21911	-16.8	4.0
51354	45045.3074	16547	13.8	1.8
51354	45337.5616	18937	45.5	3.1
60855	45698.8371	21915	-10.4	3.1
60855	47654.3590	36216	2.1	3.8
60855	47808.0710	37280	-4.0	4.1
60855	47908.9317	38036	13.4	2.3
60855	48352.5316	41308	1.7	5.9
60855	49762.4824	53906	-4.2	5.8
113120	45602.3331	21155	63.8	3.2
113120	46710.9800	29397	-14.8	4.0
113120	46920.2862	30910	-64.1	4.7
137387	46225.1106	26120	-13.2	2.4
137387	46225.3690	26129	-12.1	2.0
137387	47717.4598	36649	73.1	3.3
137387	48346.7955	41240	-23.8	3.5
152478	47270.2997	33308	-42.6	5.5
152478	47652.3252	36197	48.3	4.7
157042	46527.3127	28114	19.7	5.4
157042	46711.9244	29404	25.3	4.5
157042	46920.4479	30914	36.2	8.0
157042	49442.3921	50427	-47.3	6.8
157832	49933.1996	55410	15.1	3.3
157832	49973.0096	55913	-97.6	8.9
191610	46245.3612	26301	-16.5	2.4
191610	46337.6586	26775	10.5	8.9
191610	46337.6830	26776	17.6	10.8
191610	46337.7275	26778	17.7	7.1
191610	46337.7501	26779	11.1	8.9
191610	46337.8480	26783	16.0	9.7
191610	46337.8987	26785	16.2	15.3
191610	46338.7622	26803	19.8	6.5
191610	46338.7881	26804	18.4	5.8
191610	46338.8322	26806	17.1	9.3
191610	46338.8545	26807	11.4	13.3
191610	46338.8767	26808	26.0	7.5
191610	46692.0815	29241	8.2	5.5
191610	47790.2654	37096	10.7	16.9
191610	47790.3374	37098	8.5	4.7
191610	47791.2331	37124	15.9	10.6
191610	47791.3635	37128	21.3	16.4
191610	47791.4270	37130	3.5	11.8
191610	47791.5566	37134	14.5	5.8
191610	47791.6179	37136	8.0	13.4

Table 3—Continued

HD Number	Date (HJD-2400000)	SWP Number	V_{peak} (km s^{-1})	σ (km s^{-1})
191610	47791.7448	37140	3.3	12.1
191610	47791.8080	37142	12.4	14.7
191610	47792.0716	37148	8.4	16.5
191610	47792.2865	37150	18.2	6.5
191610	47792.4370	37154	6.7	5.9
194335	45463.4591	19938	46.3	6.5
194335	49349.8095	49705	−79.4	4.0
194335	49470.4343	50637	−96.1	9.3
194335	49686.9274	52946	29.5	3.9
214168	47691.1849	36479	−118.4	5.6
214168	47769.1105	36901	−32.9	2.3
214168	49296.6583	49099	2.3	3.6
214168	49296.7311	49102	8.3	7.3
214168	49296.7780	49104	2.4	6.5
214168	49298.6622	49130	3.0	2.8
214168	49298.7078	49132	21.2	5.3
214168	49299.6744	49145	23.4	5.8
214168	49299.7211	49147	21.6	5.0

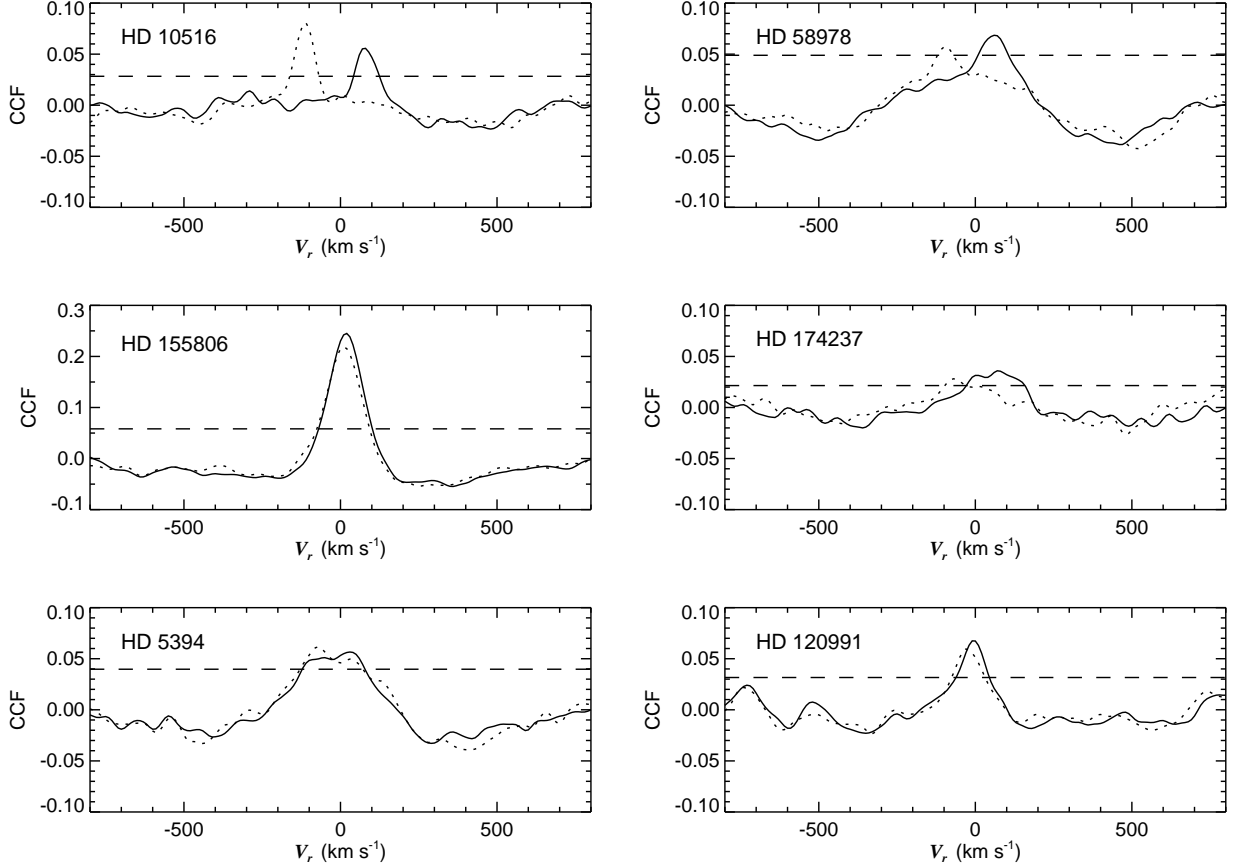


Fig. 1.— Example CCFs for two cases of hot component detection (top row) with several other cases where the peak is associated with the Be component (second and third rows). The top panels show the CCFs for HD 10516, a confirmed system with a hot subdwarf companion (Gies et al. 1998), and HD 58978, a confirmed system with a fainter subdwarf companion (Peters et al. 2008). The middle panels show how the spectrum of the emission-line star contributes more to the CCF for a hot star (HD 155806; O7.5 IIIe) than a mid-range temperature star (HD 174237; B4 IV(e)). The lower row illustrates how the CCF from the rapidly rotating Be component is usually very broad (HD 5394; $V \sin i = 432 \text{ km s}^{-1}$), but sometimes narrow (HD 120991; $V \sin i = 70 \text{ km s}^{-1}$). Examples of the CCFs for blue and red Doppler-shifted spectra are plotted as dotted and solid lines, respectively. The horizontal dashed lines indicate the $S/N=3$ limit for detection.

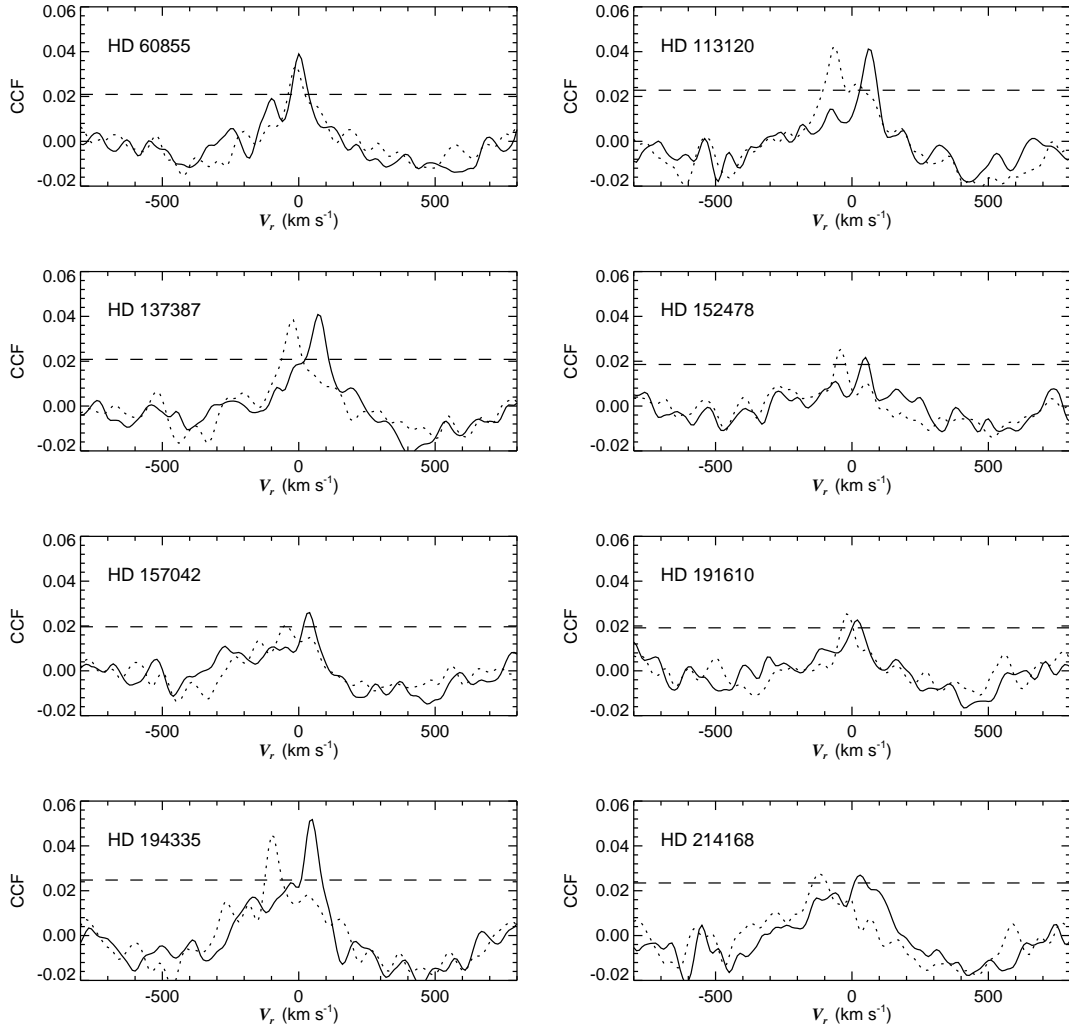


Fig. 2.— CCF plots of eight Be+sdO binary candidates in the same format as Fig. 1.

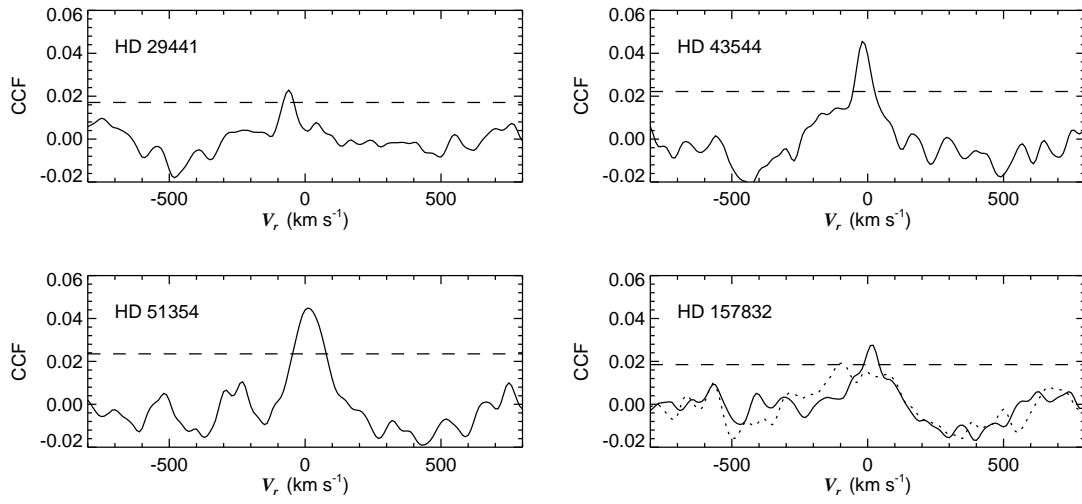


Fig. 3.— CCF plots of four potential Be+sdO binary candidates in the same format as Fig. 1.

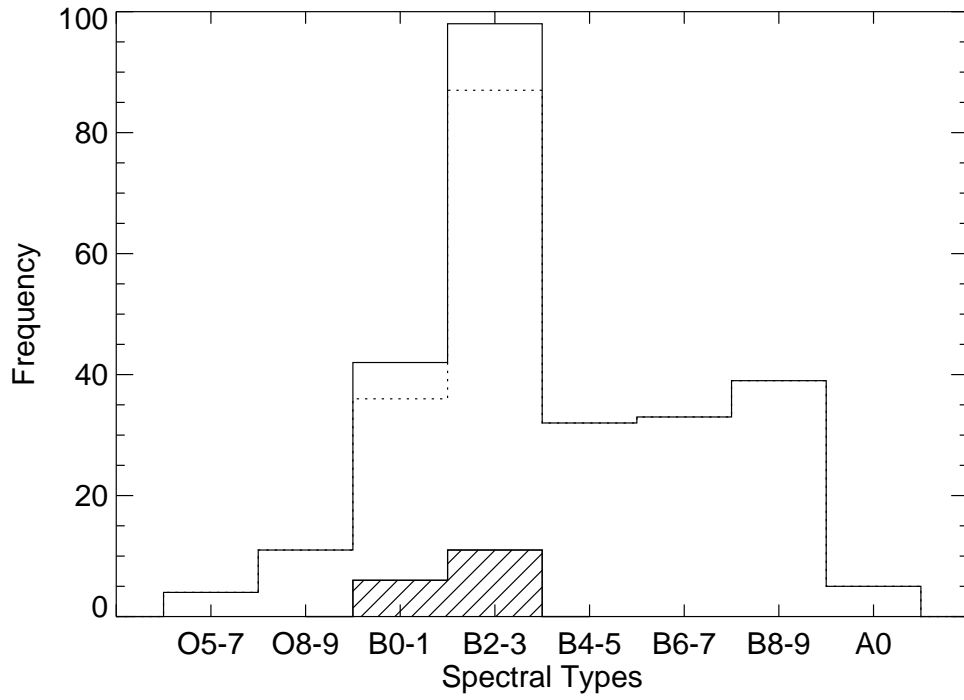


Fig. 4.— Histograms of the spectral type distributions of the full sample (solid line), those with no detections (dotted line), and those with known or candidate Be+sdO systems (line filled).